An Acad Bras Cienc (2023) 95(2): e20220680 DOI 10.1590/0001-3765202320220680
Anais da Academia Brasileira de Ciências | *Annals of the Brazilian Academy of Sciences*
Printed ISSN 0001-3765 I Online ISSN 1678-2690
www.scielo.br/aabc | www.fb.com/aabcjournal

ENGINEERING SCIENCES

Sliding Mode-Based Active Disturbance Rejection Control of Assistive Exoskeleton Device for Rehabilitation of Disabled Lower Limbs

NASIR A. ALAWAD, AMJAD J. HUMAIDI & AHMED S. ALARAJI

Abstract: In this study, a hybrid control strategy is proposed to improve the tracking performance of lower limb exoskeleton system dedicated for rehabilitation the motion of hip and knee limbs in disabled persons. The proposed controller together with exoskeleton device is practically instructive to make exercises for people suffering weakness in their lower limbs. The proposed controller combined both active disturbance rejection control (ADRC) with sliding mode control (SMC) to get their powerful characteristics in terms of rejection capability and robustness characteristics. The dynamic modelling of swinging lower limbs are developed and the controller has been designed accordingly. The numerical simulations have been conducted to validate the effectiveness of proposed controller. A comparison study in performance has been performed between the proposed controller and the traditional controller ADRC based on proportional-derivative controller. The simulated results showed that the proposed controller has better tracking performance than conventional version. In addition, the results showed that the sliding mode-based ADRC can considerably reduce the chattering level and better rejection capability, fast tracking behavior and less control effort.

Key words: Exoskeleton system, rehabilitation training, sliding mode control, ADRC, PD controller, exogenous disturbance.

INTRODUCTION AND OVERVIEW

The assistive lower-limb exoskeleton is a robot device that assists people with poor motion skills to walk and make normal motion activities. The lower-limb exoskeleton aims, through mimicking the human-like motion to enhance the lifestyle of the elderly, to improve the life quality, to enable disabled people with physical limitations such that improving their physical and mental health (Su et al. 2018).

Utilizing robotics technologies for rehabilitation applications promises to enhance the current rehabilitation standard to higher quality level. Due to high safety condition required by lower-limb exoskeleton especially for old patients, it is necessary to consider the design of robust and high precision controller for that purpose (Lin et al. 2016, Sergey et al. 2016, Zha et al. 2018).

Traditional control techniques like proportional-integral-derivative (PID) control (Kasim et al. 2019) and computed torque method (Han et al. 2018) could not cope the uncertainties in the assistive device due to different wearers and load exertions during physical exercises. In addition, these conventional control strategies have difficulty in meeting the actual requirements of patients and have limited capabilities of trajectory tracking. Recently, modern control approaches have included in the control application for rehabilitation devices to solve the problems of robustness, disturbance rejection capability and accuracy of tracking errors. As such, other control techniques have been introduced in the rehabilitation applications like model-based control (Wang et al. 2018), optimal control (Gupta et al. 2019) and backstepping control (Salman & Kadhim 2022). However, these controllers require exact model in their control design. To solve the problem of model knowledge, recent control schemes are proposed in rehabilitation applications such as the adaptive control (Sun et al. 2020), robust control (Han et al. 2020), and fuzzy control (Kwa et al. 2009), fuzzy PID control (Al Rezage & Tokhi 2016) and sliding mode control (Chen et al. 2019), and active disturbance rejection (Li et al. 2020).

In order to utilize the benefits of some control schemes, hybridization is required to combine their powerful advantages. In this study, the sliding mode controller and the active disturbance rejection control has been mixed to yield SM-based ADRC (SMADRC) for trajectory tracking of lower-limb exoskeleton system.

The sliding mode control (SMC) is widely used in robot control systems (Liu et al. 2018). The SMC does not depend on a mathematical model of the controlled system and has strong anti-interference ability and good robustness (Ahmed et al. 2019, Brahmi et al. 2021). In the analysis of SMC, the trajectory motion of system states can be divided into two parts. The first part begins from the initial condition and ends at the sliding surface or manifold. The second part represents the motion on the sliding surface until reaching the equilibrium points (Du et al. 2017). However, one critical problem which arises when the trajectory reaches the sliding surface is that it is difficult to strictly slide along the sliding surface to the equilibrium point. Instead, the system state moves back and forth across the sliding surface to approach the equilibrium point, which results in chattering (Teng & Bai 2019).

In order to ensure effective control, some control strategies assumes that all components of the state vector can be actually measured. However, in some cases, the measurements of all states are difficult to realize. Therefore, it is necessary to estimate unmeasurable states for implementation in the control system. One solution of measurement problem is to use extended state observer (ESO), which is designed to estimate a wide range of disturbances without the need of an accurate model (Huang & Xue 2014). With this observation technique, the parametric uncertainties and unmodeled dynamics of the controlled system are assigned as an additional state variable, and hence the disturbances and unmodeled dynamics can be compensated if an output feedback control approach is effectively used.

One recent and effective controller which mainly depends on the ESO is the active disturbance rejection controller (ADRC). This controller has been applied in many applications to solve many control problems (Alawad et al. 2022b, a, Humaidi & Badr 2018, Abdul-Adheem et al. 2020, 2021). The ADRC was firstly presented by Han to provide a solution for disturbances cancellation. This controller has replaced the Proportional-Integral-Derivative (PID) controller due to its superiority in performance and it could prove high efficiency in most practical applications (Han et al. 2009). In order to improve the performance of ADRC-based lower-limb exoskeleton system in terms of robustness, fast convergence and error accuracy, the ADRC has been combined with SMC to establish the "SM-based ADRC". This proposed controller could attained the characteristics of both controllers. In addition, with this hybridization, the chattering due to SMC could be eliminated due to cancellation feature of ADRC.

The main contributions of the paper are listed as follows:

1. This study has proposed sliding mode-based ADRC to improve the performance of the lower limb exoskeleton system in terms of disturbance-rejection capability and finite-time convergence.
2. The stability and global convergence property of the controlled system have been proved.
3. A comparison study have been conducted between proposed sliding mode-based ADRC and proportional derivative-based ADRC for the lower-limb exoskeleton system.

MATERIALS AND METHODS

In this section, we introduce the basic concepts behind the knee-joint mathematical model, as well as the ADRC control elements, and develop the suggested controller.

Knee-Joint Mathematical Model

The lower limb rehabilitation exoskeleton system is a multiple-degree-of-freedom open chain mechanism. It is composed of irregular links that have complex non-linearity and strong coupling characteristics (Campbell et al. 2020, Al Rezage & Tokhi 2016). These assistive robots are vulnerable to disturbances against the patient and the ground during their controlling process. Therefore, it is difficult to establish complete and accurate mathematical model of the Exoskelton devices. According to the dynamic model of the lower limb rehabilitation exoskeleton, the mathematical relationship between the motion of the hip, knee joints, and the control torque can be obtained. Ignoring the influence of environmental interference on the lower limb rehabilitation exoskeleton, a simplified structure diagram of the unilateral lower limb was established in the sagittal plane, as shown in Fig. 1.

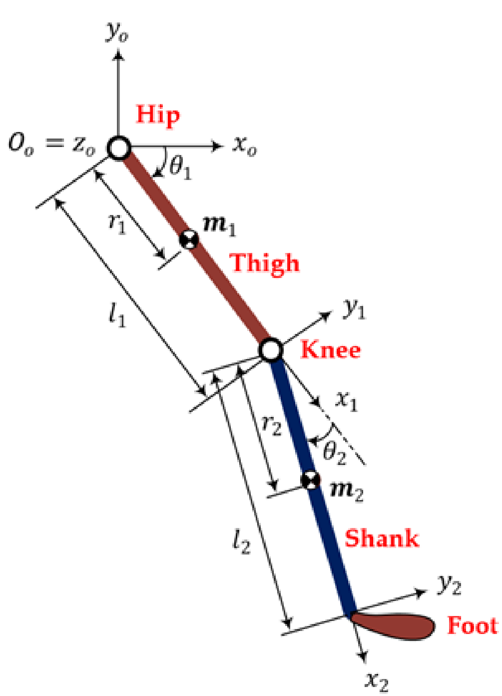

Figure 1. The schematic diagram of a wearable exoskeleton.

The Lagrange method is used to establish the dynamic model of the lower limb rehabilitation exoskeleton robot, which can be expressed by a second-order nonlinear differential Equation (Winter 2009, Craig 1986)

$$M(\theta)\ddot{\theta} + C(\theta,\dot{\theta})\dot{\theta} + G(\theta) + d(t) = u(t) \tag{1}$$

or, in matrix form Eq.(1) can be written as

$$\begin{gathered}\begin{bmatrix} M_{11} & M_{12} & M_{21} & M_{22} \end{bmatrix}\begin{bmatrix} \ddot{\theta_1} & \ddot{\theta_2} \end{bmatrix} + \begin{bmatrix} C_{11} & C_{12} & C_{21} & C_{22} \end{bmatrix}\begin{bmatrix} \dot{\theta_1} & \dot{\theta_2} \end{bmatrix} \\ + \begin{bmatrix} d_1(t) & d_2(t) \end{bmatrix} + \begin{bmatrix} G_1(\theta) & G_2(\theta) \end{bmatrix} = \begin{bmatrix} u_1(t) & u_2(t) \end{bmatrix}\end{gathered} \tag{2}$$

where θ ,$\dot{\theta}$, and $\ddot{\theta}$, respectively represent the angle, angular velocity, and acceleration of a robot in joint space. $M(\theta) \in R^{(2\times2)}$ are matrices of human limbs for each inertia. Coriolis and centrifugal torque are given by $C(\theta,\dot{\theta}) \in R^{(2\times2)}$. The torque of gravity $G(\theta) \in R^{(2\times1)}$ has one-dimensional vector . $d(t) \in R^{(2\times1)}$ is the vector of external disturbance, and $u(t) \in R^{(2\times1)}$ indicates the control signal (Han 1998). The inertial matrix $M(\theta)$ can be represented as below.

$$\begin{aligned} &M_{11}(\theta) = I_1 + I_2 + m_1 r_1^2 + m_2 L_1^2 + m_2 r_2^2 + 2m_2 r_1 r_2 cos(\theta_2) \\ &M_{12}(\theta) = M_{21}(\theta) = I_2 + m_2 r_2^2 + m_2 L_1 r_2 cos(\theta_2) \\ &M_{22}(\theta) = I_2 + m_2 r_2^2 \end{aligned} \tag{3}$$

The Coriolis and centrifugal force matrix $C(\theta)$ can be represented as followings:

$$\begin{aligned} &C_{11} = -m_2 L_1 r_2 sinsin(\theta_2)\dot{\theta}_2 \\ &C_{12} = -m_2 L_1 r_2 sinsin(\theta_2)(\dot{\theta} + \dot{\theta}_2) \\ &C_{21} = m_2 L_1 r_2 sinsin(\theta_2)\dot{\theta}_1 \\ &C_{22} = 0 \end{aligned} \tag{4}$$

The gravitational item $G(\theta)$can be represented as

$$\begin{aligned} &G_1 = m_1 r_1 g sin(\theta_1) + m_2 g L_1 sinsin(\theta_1) + m_2 g r_2 sin(\theta_1 + \theta_2) \\ &G_2 = m_2 g r_2 coscos(\theta_1 + \theta_2) \end{aligned} \tag{5}$$

In this application, the dynamic model of the exoskeleton leg is a multi-input and multi-output (MIMO) system and the above equations can be represented as follows:

$$\begin{aligned} M_{11}\ddot{\theta}_1 + M_{12}\ddot{\theta}_1 + C_{11}\theta_1 + C_{12}\dot{\theta}_2 + G_1 + D_1 = \tau_1 \\ M_{21}\ddot{\theta}_1 + M_{22}\ddot{\theta}_2 + C_{21}\theta_1 + C_{22}\dot{\theta}_2 + G_2 + D_2 = \tau_2 \end{aligned} \tag{6}$$

where, τ_1 and τ_2 represent the actuating torques for hip and knee, respectively. The numerical values of these physical parameters are defined and listed in Table I.

ADRC for Lower Limb Exoskeleton

The magic with ADRC is that it has the capability to compensate model uncertainties and external disturbances by introducing extended state observer to achieve this objective. Without loss of generality, the concept of ADRC can be analyzed by considering a second-order nonlinear system

$$\ddot{\theta} = \ddot{y} = f(t,\theta,\dot{\theta},w) + bu \tag{7}$$

Table I. The variables definition for Lower wearable exoskeleton [25].

Parameters	Definitions	Units	values
L_1	Hip Length	m	0.54
L_2	Knee Length	m	0.48
r_1	center of Hip mass	m	0.2338
r_2	center of Knee mass	m	0.241
m_1	Hip Mass	Kg	8
m_2	Knee Mass	Kg	3.72
I_1	Hip Inertia	Kg.m2	0.42
I_2	Knee Inertia	Kg.m2	0.07
g	Gravity	m/s2	9.8
θ_{1d}	Angular Displacement of Hip	Rad	-
θ_{2d}	Angular Displacement of Knee	Rad	-
$\dot{\theta}_1$	Angular Velocity of Hip	Rad/s	-
$\dot{\theta}_2$	Angular Velocity of Knee	Rad/s	-
$\ddot{\theta}$	Angular acceleration	Rad/s2	-

In state-space form, the above equation can be written as:

$$
\begin{aligned}
\dot{x_1} &= x_2 \\
\dot{x_2} &= x_3 + bu \\
\dot{x_3} &= \dot{f} \\
y &= x_1
\end{aligned}
$$

where,θ is the state variable to be controlled, b is a boundary that is generally known. The term f accounts for the combined effect of internal and external disturbances w. In this case, the state space has been extended to third order, where the third state variable represents lumped uncertainties.

In order to estimate all states of extended system, including the lumped uncertainties, an extended state observer (ESO), which is part of ADRC structure, is utilized for this task that permits estimation with adequate accuracy. In other words, the ESO will estimate f and the other states of the system,x_1 and x_2, which corresponds estimate $(y, \dot{y}, ..., f)$ in the original dynamic system. The suggested observer for extended dynamic system, described by Eq. (7), takes the form of linear Luenberger-like estimator which was widely used in the literature (Campbell et al. 2020, Al Rezage & Tokhi 2016)

$$
\begin{aligned}
\dot{\hat{z}} &= A\hat{z} + bu + L(z - \hat{z}) \\
\hat{y} &= C\hat{z}
\end{aligned} \tag{8}
$$

where, $\hat{z} = \begin{bmatrix} \hat{z}_1 & \hat{z}_2 & \hat{z}_3 \end{bmatrix}^T$ is the vectors of estimates of y, $\dot{y}$, and f, respectively. When properly designed and implemented, the state of the state estimates of observer, represented by Eq. (8), will track that of plant represented by Eq. (6). The elements of vector L can be obtained, for example, based on pole-placement technique (Winter 2009). It is easy to find the characteristics equation for ESO:

$$Q(s) = |sI - (A - LC)| \tag{9}$$

One can place the roots of characteristic equation at negative real axis in the complex plane and these roots may be chosen in terms of observer's bandwidth ω_0; that is $Q(s) = (s + \omega_0)^3$. According to this argument, the gains of observer vector as follows:

$$L = \begin{bmatrix} 3\omega_0 & 3\omega_0^2 & \omega_0^3 \end{bmatrix}$$

Based on ESO, the term f is estimated; that is $x_3 \approx f$. If the control law is defined by

$$u = ((u_0 - f))/b \tag{10}$$

Then, Eq.(6) becomes $\ddot{y} = u_0$. This results in an approximate double integral plant. The PD controller can be proposed to generate the control signal u_0 as follows:

$$u_0 = K_p(y_d - \hat{z}_1) + K_d(\dot{y}_d - \hat{z}_2) \tag{11}$$

where u_0 is the output of the PD controller. Then, according to Eq.(10), the control law can be rewritten as

$$u = ([K_p(y_d - \hat{z}_1) + K_d(\dot{y}_d - \hat{z}_2) - f])/b \tag{12}$$

It is clear that the objective of ADRC is to continuously compensate the lumped uncertainty f and works to cancel it out. For tuning the design parameters of PD controller K_p and K_d, one may use the bandwidth of the system ω_c to determine these terms (Alawad et al. 2022a, Han 1998, Chen et al. 2011)

$$k_p = \omega_c^2 \quad k_d = 2\omega_c \tag{13}$$

This related to design specifications, specially the settling time T_s, so that

$$\omega_c = 10/T_s \tag{14}$$

In this study, if one selects $T_s = 0.4s$, then $\omega_c = 24.5 rad/sec$ and the value of observer bandwidth (ω_0) is calculated as

$$\omega_0 = 4\omega_c \tag{15}$$

Figure (2) shows the active rejection disturbance based on proportional derivative controller.

Proposed Controller of SM-based ADRC

In general, the SMC for systems can be achieved by the sliding surface definition and the control law design. The proposed control approach aims at improving the whole performance with high accuracy and fast coverage. The tracking error in the non-linear SMC strategy can converge to zero in finite time (Quao & Zhang 2017, 2020).

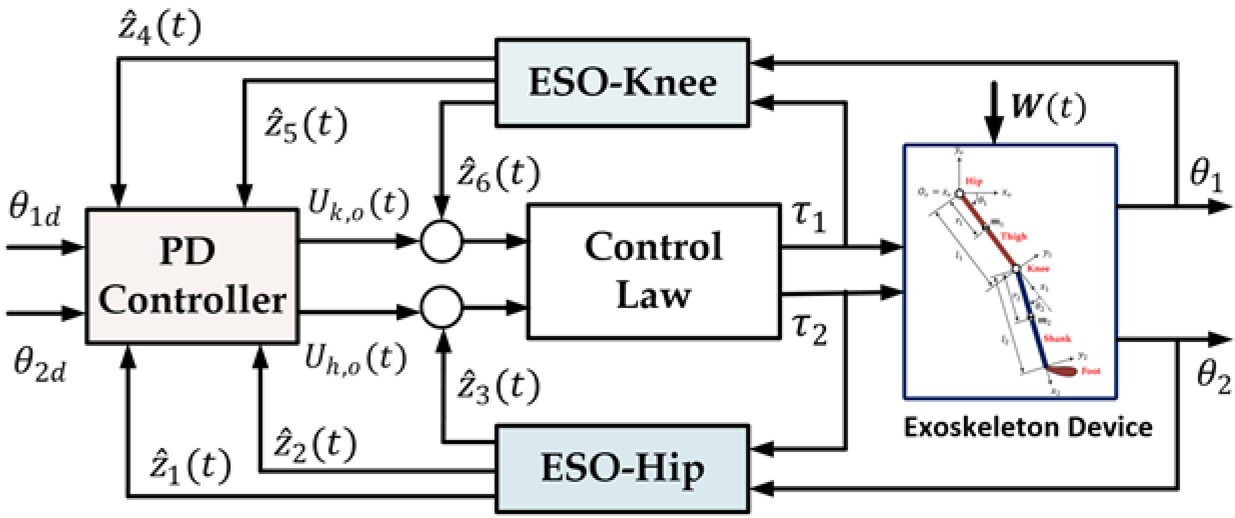

Figure 2. Configuration of the simulation for the 2-DOF lower limb exoskeleton (PD-based ADRC).

The tracking errors (e_1,e_2) represents the difference between the desired angular positions (θ_{1d},θ_{2d}) and the actual angular positions (θ_1,θ_1) for the hip and knee joints, respectively,

$$e = \theta_d - \theta = \begin{bmatrix} \theta_{1d} - \theta_1 & \theta_{2d} - \theta_2 \end{bmatrix}^T \tag{16}$$

where, θ_{1d} and θ_{2d} denotes the desired trajectories for hip and knee joint, respectively, while θ_1 and θ_2 denotes the actual angular positions for hip and knee joint, respectively. To ensure that the tracking errors converge within finite-time and to avoid the singularity problem, the sliding mode surface can be designed as (Wang et al. 2021)

$$s = \dot{e} + ce \tag{17}$$

where, $s = \begin{bmatrix} s_1 & s_2 \end{bmatrix}^T$ includes the sliding surface components for each channel of control; that is for hip joint and knee joint. The coefficient c is a real positive number ($c > 0$). Due to unmodeled system dynamic and sensor noises, the extended states observer may fail to enforce the estimated state $\hat{z}_3$ tracking the actual state z_3 precisely. Therefore, an estimation error $\bar{z}_3$ may arise, which can be expressed by:

$$|\bar{z}_3| = |\hat{z}_3 - z_3| = |\hat{f} - f| \leq \Delta_f \tag{18}$$

where Δ_f is the upper bound of estimation error $|\bar{z}_3|$. Since $e = \theta_d - \theta$, the control input of SM-based ADRC can be designed as:

$$u = (-\hat{z}_3 + u_0)/b \tag{19}$$

$$u_0 = (|\ddot{\theta}_d| + \Delta_f + c|\dot{e}|).sign(s) \tag{20}$$

Taking the time derivative of sliding surface of Eq. (17) to obtain

$$\dot{s} = \ddot{e} + c\dot{e} \tag{21}$$

Using Eq. (21) and Eq.(16) to get

$$\dot{s} = \ddot{\theta}_d - \ddot{\theta} + c\dot{e} \tag{22}$$

According to Eq.(7)

$$\ddot{\theta} = f + bu = f + b(-\hat{z}_3 + u_0)/b \tag{23}$$

$$\ddot{\theta} = f - \hat{f} + |\ddot{\theta}_d| + \Delta_f + c|\dot{e}|)sign(s) \tag{24}$$

STABILITY ANALYSIS

One of the main issues in control system design is how to guarantee stability of the controlled system (Sun et al. 2017). In this part, the stability analysis will be conducted based on Lyapunov theory. Lemma 1: Considering the system of Eq. (7) with the parametric uncertainties f, the control law developed based on SM-based ADRC can lead to asymptotic convergence of tracking error to zero for a given desired trajectory. The stability analysis of the proposed control algorithm is initiated by choosing a Lyapunov function candidate with positive definite property, which depend on sliding surface

$$V(s) = 1/2s^2 \tag{25}$$

The time derivative of Eq. (25) can be given as

$$\dot{V} = s\dot{s} \tag{26}$$

Taking the time derivative of Lyapunov function to have

$$\begin{aligned}\dot{V} &= s\dot{s}\\ &= s(\ddot{\theta}_d - \ddot{\theta} + c\dot{e})\\ &= s(\ddot{\theta}_d - f + \hat{f} - (|\ddot{\theta}_d| + \Delta_f + c|\dot{e}|)sign(s) + c\dot{e})\\ &= s\ddot{\theta}_d + c\dot{e}s + (\hat{f} - f)s - |\ddot{\theta}_d||s| - \Delta_f|s| - c|\dot{e}||s|)\end{aligned} \tag{27}$$

or,

$$\dot{V} = (s\ddot{\theta}_d - |\ddot{\theta}_d||s|) + [(\hat{f} - f)s - \Delta_f|s|] + (c\dot{e}s - c|\dot{e}||s|) \tag{28}$$

Using the following inequalities

$$\begin{aligned}s\ddot{\theta}_d &< |s||\ddot{\theta}_d|\\ s(f - \ddot{f}) &< |s|\Delta_f\\ cs\dot{e} &< c|s||\dot{e}|\end{aligned} \tag{29}$$

Then, based on the above assumptions, one can conclude that

$$\dot{V} = (s\ddot{\theta}_d - |\ddot{\theta}_d||s|) + [(\hat{f} - f)s - \Delta_f|s|] + (c\dot{e}s - c|\dot{e}||s|) < 0 \tag{30}$$

Figure 3 shows the schematic representation of SM-based ADRC for the Hip-and-Knee Exoskeleton system for rehabilitation.

NUMERICAL SIMULATIONS AND COMPARATIVE ANALYSIS

To demonstrate the advantages and superiority of the proposed SMCADRC, a PD-based active disturbance rejection controller (PDADRC) are also designed for comparison purpose. The design

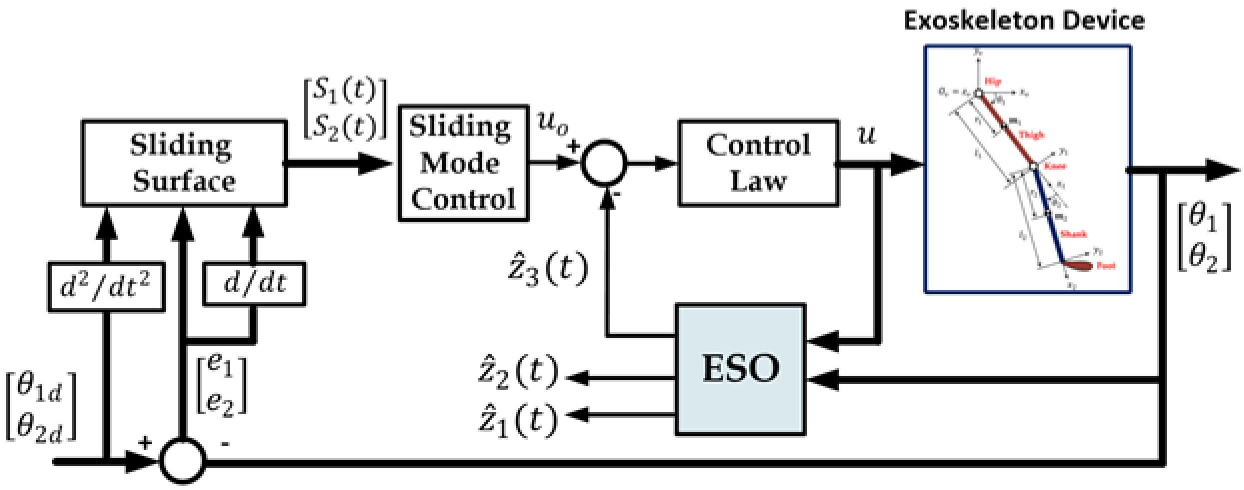

Figure 3. Configuration of the simulation for the 2-DOF lower limb exoskeleton (SM-based ADRC).

results of these two controllers are given directly for simplicity. If one chooses the bandwidth of observer ω_0 to be equal to $\omega_0 = 4\omega_c$, then it easy to calculate the elements of observer matrix gains (L_1, L_2, L_3) according to Eq.9. For a fair comparison, assume that the observers and controller gains were the same in both techniques (PDADRC) and (SMCADRC). Allow for a settling time of 0.4 seconds and $\omega_c = 24.5 rad/sec$ in the design. Two controllers are designed using Eq.11 for (PDADRC) and Eq.20 for (SMCADRC). MATALAB's Simulink is used to carry out the numerical simulations. Whereas the SMC parameters are determined through trial and error adjustment. The SMC controller gains are set to $K_1 = 20$, $c_1 = 0.1$ for hip joint and $K_2 = 100$, $c_2 = 0.01$ for knee joint. The controller's gains of (PDADRC) are $k_p = 600, k_d = 49$ for both links. Some of the performance indicators used to measure tracking accuracy include the integral of the absolute error (IAE), the integral square error (ISE), the integral absolute of the control signal (IAU), and the Root Mean Square Error (R.M.S.E) (Alawad et al. 2022b, Abdul-Adheem et al. 2020, Neto et al. 2021).There are two test, one for normal case(without disturbances) and the other for disturbance case. The clinical gait analysis determines the desired hip and knee joint trajectories (CGA). The following fitting functions can be obtained as a result of this (Li et al. 2020):

$$\theta_{1d} = 0.66sin(0.0665t + 0.282) + 0.361sin(3.69t + 1.17) + 0.0412sin(8.32t - 0.4631)$$

$$\theta_{2d} = 0.761sin(0.774t - 3.25) + 1.98sin(6.55t - 0.326) + 2.22sin(6.33t - 3.35)$$

where t is the real time which ranges from 0 to 8 seconds. In this part, the effectiveness of proposed SM-based ADRC has been tested and verified via numerical simulation. In addition, tracking performance of proposed controller has been compared to that based on PD-based ADRC in different exertion of disturbance.

Scenario I: Disturbance-Free Condition

In this scenario, the SM-based ADRC and PD-based ADRC have been tested and evaluated under no-disturbance condition, where $d(t) = 0$ for both joints. Fig. 4 and Fig. 5 show, respectively, the

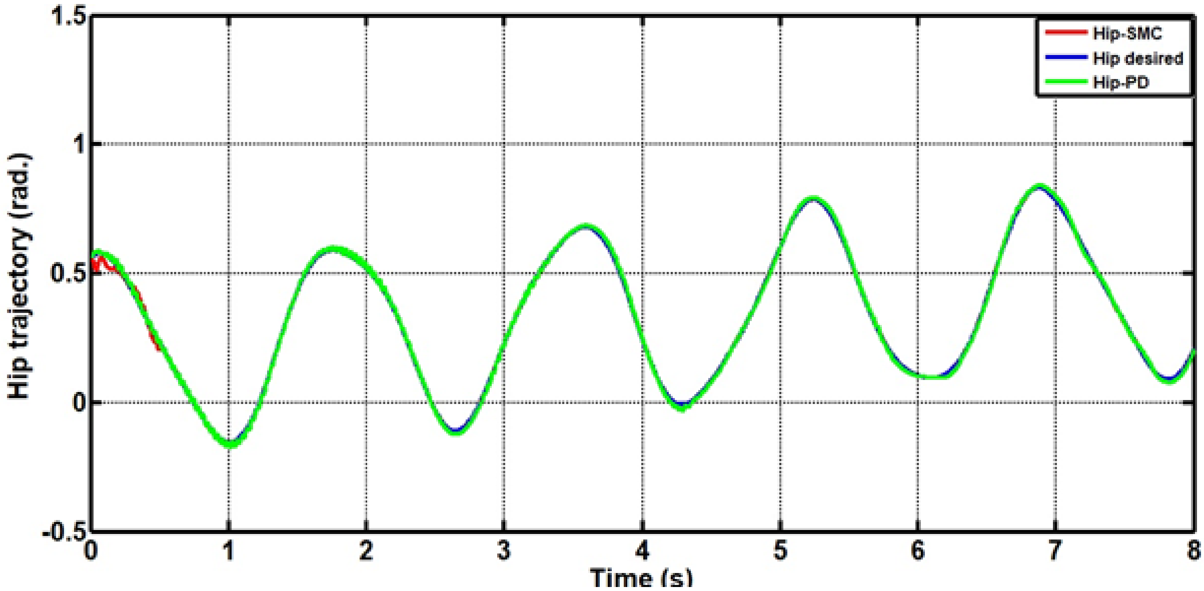

Figure 4. Time response of hip position joint for both controllers without disturbance.

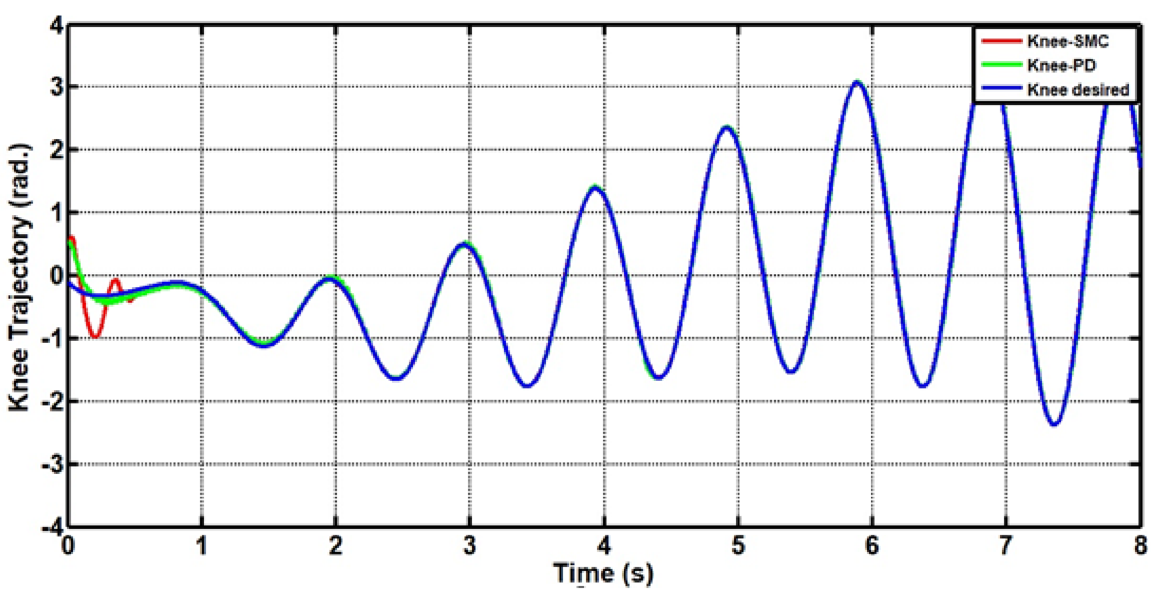

Figure 5. Time response of knee position joint for both controllers without disturbance.

trajectory tracking performance of SM-based ADRC and PD-based ADRC for the hip and knee joints. As shown in Fig. 4 and Fig. 5, the trajectory tracking due to SM-ADRC has better tracking accuracy than that based on PD-based ADRC. However, the SM-based ADRC showed degradation in transient behavior at startup simulation as compared to transient characteristics due to PD-based ADRC. This can be further clarified in error figures indicated in Fig. 6 and Fig. 7. It is clear from the figures that there is bad transient behaviour for controlled system based on proposed controller, while there is good transient characteristics due to PD-based ADRC for both hip and knee joints. It is worthy to mention that the oscillatory behaviours of angular positions for both joints due to both controllers are not due to unstable characteristics of controllers, but due to the behaviours of desired trajectories.

The well-performance of trajectory tracking is the proof of stability for both controller. Moreover, it is evident from Fig. 6 and Fig. 7 that the steady state-errors due to SM-based ADRC is considerably less than that based on PD-based ADRC for both joints. In addition, the PD-based ADRC showed high chattering at the error signals, while this chattering behavior has disappeared in the case of SM-based ADRC. The numerical evaluation of dynamic performance for both controllers and for joints in Table II. Two indices have been used to evaluate the tracking error; one based on Root Mean Square of Error (RMSE) and Integral of Absolute of Error (IAE). The table shows that less RMSE has been given by SM-based ADRC than that resulting from PD-based ADRC. However, the table reports the numerical value of control efforts resulting from both controllers for both hip and knee joints. It is evident that the SM-based ADRC generates higher control effort than that based on PD-based ADRC. This is the price which has to be paid by the proposed controller to improve the tracking errors. Moreover, the chattering behavior resulting from PD-ADRC is higher than that based on SM-based ADRC. In other words, the SM-based ADRC shows smoother response than that based on PD-based ADRC.

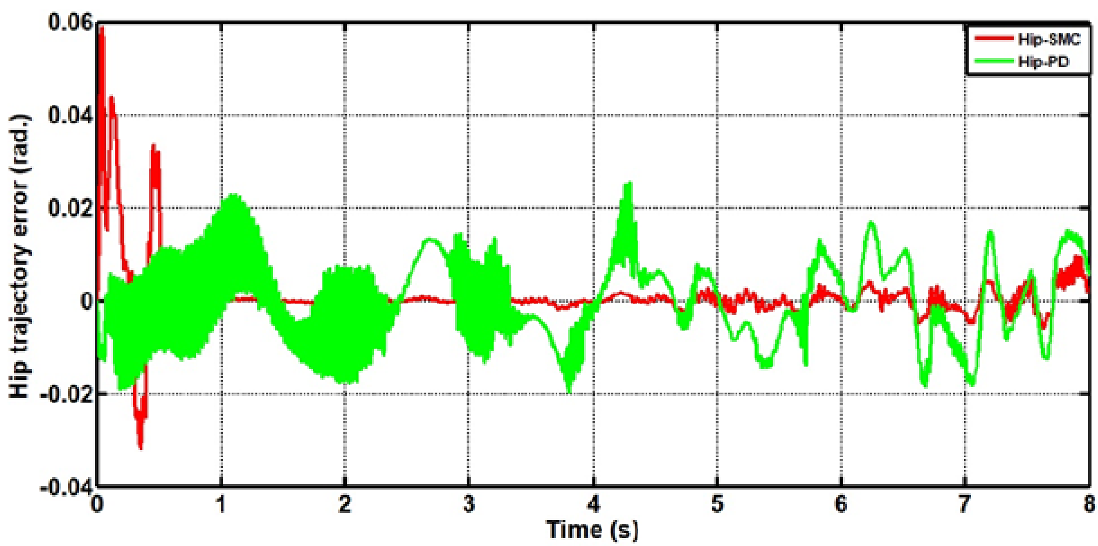

Figure 6. **Tracking error of hip position joint for both controllers without disturbance.**

Table II. **Performance indices of ADRC without disturbance for both joints.**

Control Method	R.M.S.E (rad.)	IAE (rad.)	ISE (rad.)	IAU (N.m)
PDADRC for hip	0.0894	0.0598	0.0006	787.9
SMCADRC for hip	0.0107	0.0772	0.0032	698.8
PDADRC for knee	0.1022	0.3495	0.04432	249.1
SMCADRC for knee	0.0541	0.1744	0.0799	377.4

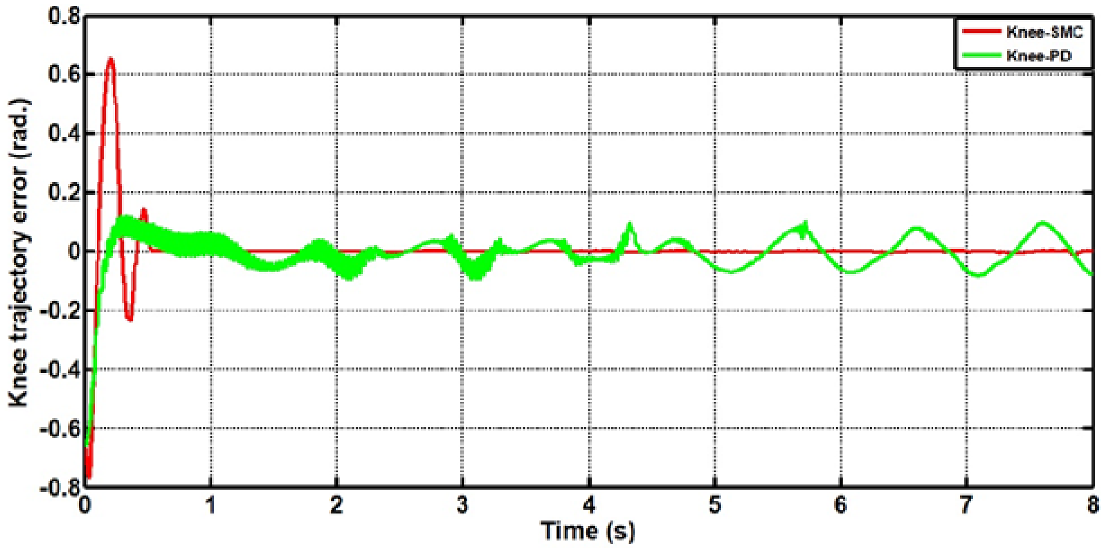

Figure 7. Tracking error of knee position joint for both controllers without disturbance.

Scenario II: Disturbance-Application Condition

In this scenario, the performance of the proposed controller is assessed under disturbance application, where $d(t) \neq 0$. The scenario has been splitted into cases; one case considered the disturbance application on the hip joint and the other case considered the disturbance exertion on the knee joint.

- Case I: In this case, a disturbance value of $d_1(t) = 0.5kg$ has been applied at the output of hip joint at the start of the flexion/extension cycle (at time=2 sec). The controllers have been tested with desired trajectory. Fig. 8 shows the trajectory tracking performance of both controllers for the hip joint. Fig. 9 shows the error behavior for hip joint. As indicated in Fig. 8, the response due to both controllers have affected upon disturbance exertion, but the response based on SM-based ADRC shows better disturbance rejection capability than that based on PD-based ADRC. The SM-based ADRC could successfully compensate the disturbance in shorter time and has better transient characteristics than the PD-based ADRC. According to Fig. 9 and Table III, one can deduce that the RMSE resulting from SM-ADRC is less than that due to PD-based ADRC. However, the improvement of error accuracy obtained by proposed controller is on the price of higher control effort to be produced by controller. In other words, the control efforts produced by SM-based ADRC is higher than conventional controller.

- Case II: In this case, a disturbance value of $d_1(t) = 0.5kg$ has been applied at the output of knee joint at the start of the flexion/extension cycle (at time=2 sec). The performances of controllers have been assessed when subjected to the same desired trajectory. Fig. 10 and Fig. 11 show the tracking performances and error behaviours based on both controllers for the knee joint, respectively. According to the figures, it is clear that the responses have been affected and distorted upon disturbance application. However, the response due to SM-based ADRC shows better disturbance rejection capability than that based on PD-based ADRC. The SM-based ADRC could successfully compensate the disturbance in shorter time and has better transient

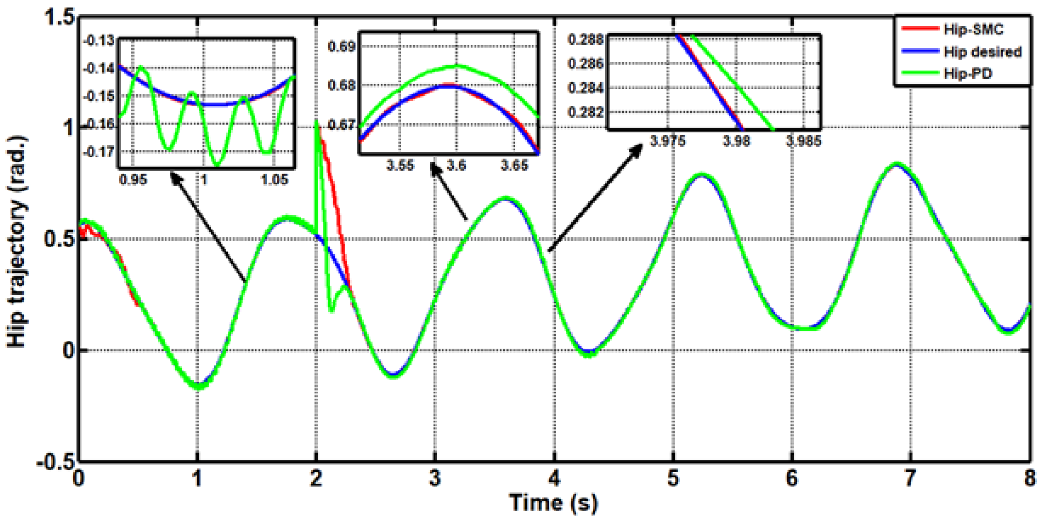

Figure 8. Time response of hip position joint for both controllers with load disturbance.

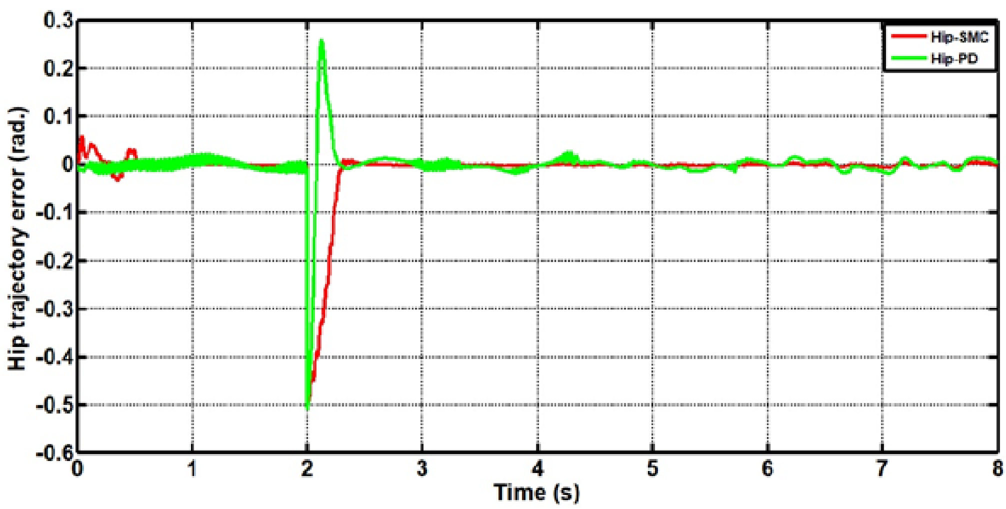

nbm

Figure 9. Tracking error of hip position joint for both controllers with load disturbance.

Table III. Performance indices of ADRC with load disturbance at hip joint.

Control Method	R.M.S.E(rad.)	IAE(rad.)	ISE(rad.)	IAU(N.m)
PDADRC for hip	0.0435	0.1055	0.0139	757.5
SMCADRC for hip	0.0361	0.1587	0.0375	687.1
PDADRC for knee	0.1828	0.6104	0.2319	242.6
SMCADRC for knee	0.0578	0.1889	0.0806	380.7

characteristics than that based on PD-based ADRC. In addition, the proposed controller has better noise rejection capability than its counterpart. Table IV reports the numeric performances of both controllers and one can conclude that the SM-ADRC shows better tracking error accuracy than PD-ADRC. However, the control efforts produced by the SM-based ADRC is higher than that given by the conventional controller and this is the price to be paid by proposed controller for improvement.

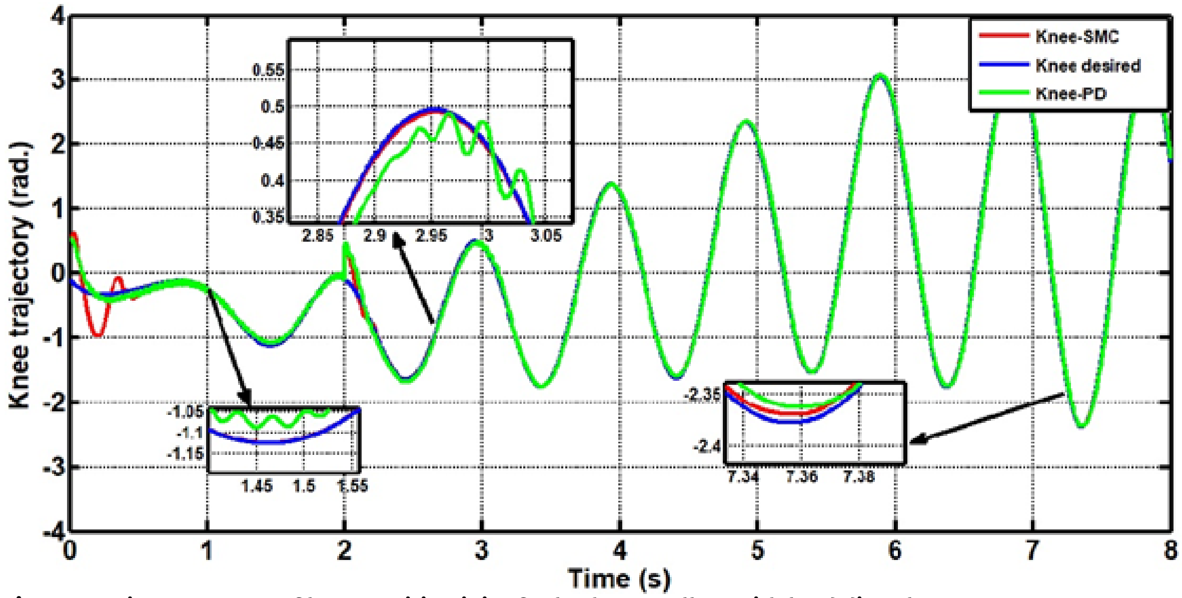

Figure 10. Time response of knee position joint for both controllers with load disturbance.

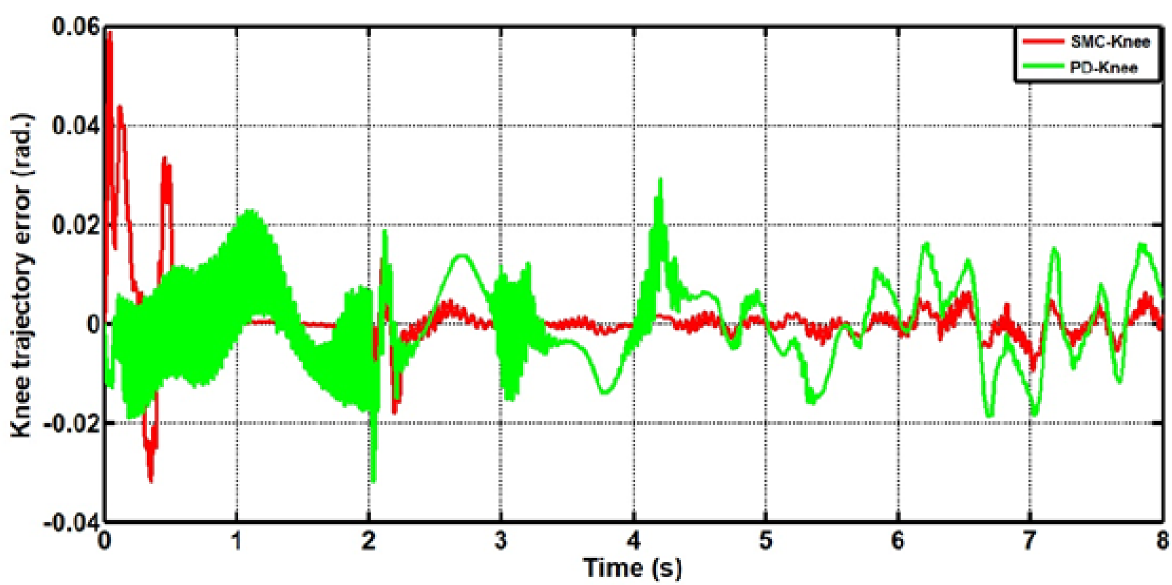

Figure 11. Tracking error of knee position joint for both controllers with load disturbance.

CONCLUSION

This study proposed SM-based ADRC for trajectory tracking of rehabilitation exoskeleton device for two degree of freedom swinging leg. The ESO is synthesized to estimate the disturbances and dynamics unknown uncertainty online and then the estimated uncertainty is utilized by proposed controller for

Table IV. Performance indices of ADRC with load disturbance at knee joint.

Control Method	R.M.S.E(rad.)	IAE(rad.)	ISE(rad.)	IAU(N.m)
PDADRC for hip	0.0892	0.0589	0.0006	709.5
SMCADRC for hip	0.0107	0.0761	0.0033	667.7
PDADRC for knee	0.1141	0.4056	0.0638	223.4
SMCADRC for knee	0.0591	0.2148	0.0910	380.7

compensating and cancellation of lumped uncertainties. The stability of the medical device controlled by the proposed controller has been proved based on Lyapunov theory. A comparison study in performance has been conducted between the proposed controller and the PD-based ADRC. The numerical simulation showed that the proposed control strategy can achieve better performance in terms of tracking accuracy and robustness characteristics as compared to PD-based ADRC. In addition, the SM-based ADRC showed better disturbance rejection capability and fast convergence rate of tracking errors as compared to conventional controller. Furthermore, the simulated results showed that the control torques required for actuating the hip limb is higher than that required for actuating the knee joint.

This study can be extended for further work by implementing the proposed control algorithm in real-time environment either using LabVIEW programming software or embedded hardware design like the FPGA (Mostafa et al. 2021). Other extension of this study is to use modern optimization methods for tuning the design parameters to have optimal performance of proposed controller (Rasheed 2020, Al-Qassar et al. 2021a, b). Also, the proposed controller can be compared in performance to other control schemes (Mahdi et al. 2022, Hameed et al. 2019, Amjad et al. 2019).

REFERENCES

ABDUL-ADHEEM WR, AZAR AT, IBRAHEEM IK & HUMAIDI AJ. 2020. Novel Active Disturbance Rejection Control Based on Nested Linear Extended State Observers. Appl Sci 10: 1-27. doi: 10.3390/app10124069.

ABDUL-ADHEEM WR, IBRAHEEM IK, HUMAIDI AJ & AZAR TA. 2021. Model-free active input–output feedback linearization of a single-link flexible joint manipulator: An improved active disturbance rejection control approach. Meas Control 4: 856-871. doi: 10.1177/0020294020917171.

AHMED SF, RAZA Y, MAHDI HF, MUHAMAD WMW, JOYO MK, SHAH A & KOONDHAR MY. 2019. Review on sliding mode controller and its modified types for rehabilitation robots. In: Proceedings of the 2019 IEEE 6th International Conference on Engineering Technologies and Applied Sciences (ICETAS), Kuala Lumpur, p. 1-8. doi: 10.1109/ICETAS48360.2019.9117390.

AL REZAGE G & TOKHI MO. 2016. Fuzzy PID Control of Lower Limb Exoskeleton for Elderly Mobility. 2016 20th IEEE Int Conf Autom Qual Testing Robot, p. 1-6. doi: 10.1109/AQTR.2016.7501310.

ALAWAD NA, AMJAD JH & AL-ARAJI AS. 2022a. Improved active disturbance rejection control for the knee joint motion model. Math Model Eng Prob 9(2): 477-483. doi: 10.18280/mmep.090225.

ALAWAD NA, HUMAIDI AJ, AL-OBAIDI ASM & ALARAJ AS. 2022b. Active Disturbance Rejection Control of Wearable LowerLimb System Based on Reduced ESO. Indones J Sci Technol 7(2): 203-218.

AL-QASSAR AA, ABDULKAREEM AI, HUMAIDI AJ, IBRAHEEM IK, AZAR TA & HAMEED AH. 2021a. Grey-wolf optimization better enhances the dynamic performance of roll motion for tail-sitter VTOL aircraft guided and controlled by STSMC. J Eng Sci Technol 16(3): 1932-1950.

AL-QASSAR AA, AL-OBAIDI ASM, HASAN AF, HUMAIDI AJ, NASSER AR, ALKHAYYAT A & IBRAHEEM IK. 2021b. Finite-Time Control of Wing-Rock Motion for Delta Wing Aircraft Based on Whale-Optimization Algorithm. Indones J Sci Technol 6: 441-456.

AMIRI MS, RAMLI R & IBRAHIM MF. 2019. Hybrid design of PID controller for four DoF lower limb exoskeleton. Appl Math Model 72: 17-27. doi: 10.1016/j.apm.2019.03.002.

BRAHMI B, BOJOIEAMI IE, SAAD M, DRISCOLL M, ZEMAM S & LARAKI MH. 2021. Enhancement of sliding mode control performance for perturbed and unperturbed nonlinear systems: Theory and experimentation on rehabilitation robot. J Electr Eng Technol 16: 599-616. doi: 10.1007/s42835-020-00615-2.

CAMPBELL SM, DIDUCH CP & SENSINGER JW. 2020. Autonomous Assistance-as-needed control of a lower limb exoskeleton with guaranteed stability. IEEE Access 8: 51168-51178. doi: 10.1109/ACCESS.2020.2973373.

CHEN CF, DU ZJ, HE LONG, WANG JQ, WU DM & DONG W. 2019. Active Disturbance Rejection with Fast Terminal Sliding Mode Control for a Lower Limb Exoskeleton in Swing Phase. IEEE Access 7: 72343-72357. doi: 10.1109/ACCESS.2019.2918721.

CHEN X, LI D, GAO Z & WANG C. 2011. Tuning method for second-order active disturbance rejection control. In: Proceedings of the 30th Chinese control conference, p. 6322-6327.

CRAIG JJ. 1986. Introduction to Robotics: Mechanics and Control. New York: Pearson Education.

DU F, SUN Y, LI G, JIANG G, KONG J, JIANG D & LI Z. 2017. Adaptive fuzzy sliding mode control algorithm simulation for 2-DOF articulated robot. Int J Wirel Mob Comput 13: 306-313.

GUPTA J, DATTA R, SHARMA AK, SEGEV A & BHATTACHARYA B. 2019. Evolutionary Computation for Optimal LQR Weighting Matrices for Lower Limb Exoskeleton Feedback Control. In: 2019 IEEE International Conference on Computational Science and Engineering (CSE) and IEEE International Conference on Embedded and Ubiquitous Computing (EUC), New York, USA, p. 24-29. doi: 10.1109/CSE/EUC.2019.00014.

HAMEED AH, AL-DUJAILI AQ, HUMAIDI AJ & HUSSEIN HA. 2019. Design of terminal sliding position control for electronic throttle valve system: A performance comparative study. Int Rev Autom Control 12: 251-260. doi: 10.15866/ireaco.v12i5.16556.

HAN JQ. 1998. Active disturbance rejection controller and its applications. Control Decis 13(1): 19-23.

HAN JQ. 2009. From PID to active disturbance rejection control. IEEE Trans Ind Electron 56(3): 900-906. doi: 10.1109/TIE.2008.2011621.

HAN S, WANG H & TIAN Y. 2018. Adaptive computed torque control based on RBF network for a lower limb exoskeleton. In: Proceedings of the 2018 IEEE 15th International Workshop on Advanced Motion Control (AMC), Tokyo, Japan, p. 35-40. doi: 10.1109/AMC.2019.8371059.

HAN S, WANG H, TIAN Y & CHRISTOV N. 2020. Time-delay estimation based computed torque control with robust adaptive RBF neural network compensator for a rehabilitation exoskeleton. ISA Trans 97: 171-181. doi: 10.1016/j.isatra.2019.07.030.

HUANG Y & XUE W. 2014. Active disturbance rejection control: Methodology and theoretical analysis. ISA Trans 53(4): 963-976. doi: 10.1016/j.isatra.2014.03.003.

HUMAIDI AJ & BADR HM. 2018. Linear and Nonlinear Active Disturbance Rejection Controllers for single-link flexible joint robot manipulator based on PSO tuner. J Eng Sci Technol Rev 11(3): 133-138.

HUMAIDI AJ & HAMEED AH. 2019. Design and comparative study of advanced adaptive control schemes for position control of electronic throttle valve. Information 10: 1-14. doi: 10.3390/info10020065.

KASIM MQ, HASSAN RF, HUMAIDI AJ, ABDULKAREEM AI, NASSER AR & ALKHAYYAT A. 2021.Control Algorithm of Five-Level Asymmetric Stacked Converter Based on Xilinx System Generator. In: Proceedings of the IEEE 9th Conference on Systems, Process and Control (ICSPC 2021), p. 174-179. doi: 10.1109/ICSPC53359.2021.9689173.

KWA HK, NOORDEN JH, MISSEL M, CRAIG T, PRATT JE & NEUHAUS PETER. 2009. Development of the IHMC mobility assist exoskeleton. In: Proc IEEE Int Conf Robot Automat, p. 2556-2562. doi: 10.1109/ROBOT.2009.5152394.

LI Z, GUAN X, LI Y & XU C. 2020. Fuzzy active disturbance rejection control for Direct Driven Exoskeleton of Swing leg. In: 2020 5th International Conference on Advanced Robotics and Mechatronics (ICARM), p. 234-239. doi: 10.1109/ICARM49381.2020.9195378.

LIN CW, SU SF & CHEN MC. 2016. Indirect adaptive fuzzy decoupling control with a lower limb exoskeleton. In: Proceedings of the IEEE 2016 International Conference on Advanced Robotics and Intelligent Systems (ARIS), Taipei, Taiwan, p. 1-5.

LIU J, ZHANG Y, WANG J & CHEN W. 2018. Adaptive sliding mode control for a lower-limb exoskeleton rehabilitation robot. In: Proceedings of the 2018 13th IEEE Conference on Industrial Electronics and Applications (ICIEA), Wuhan, China, p. 1481-1486. doi: 10.1109/ICIEA.2018.8397943.

MAHDI SM, YOUSIF SQ, OGLAH AA, SADIQ ME, HUMAIDI AJ & AZAR AT. 2022. Adaptive Synergetic Motion Control for Wearable Knee-Assistive System: A Rehabilitation of Disabled Patients. Actuators 11: 1-19. doi: 10.3390/act11070176.

NETO DLA, DANTAS AFOA, ALMEIDA TF, DE LIMA JÁ & MORYA E. 2021.Comparison of Controller's Performance for a Knee Joint model based on Functional Electrical Stimulation Input. In: International IEEE/EMBS Conference on Neural Engineering (NER) Virtual Conference, p. 836-839.

QIAO L & ZHANG W. 2017. Adaptive non-singular integral terminal sliding mode tracking control for autonomous underwater vehicles. IET Control Theory Appl 11(8): 1293-1306. doi: 10.1049/iet-cta.2017.0016.

QIAO L & ZHANG W. 2020. Trajectory tracking control of AUVs via adaptive fast nonsingular integral terminal sliding mode control. IEEE Trans Ind Informat 16(2): 1248-1258. doi: 10.1109/TII.2019.2949007.

RASHEED LT. 2020. Optimal tuning of linear quadratic regulator controller using ant colony optimization algorithm for position control of a permanent magnet dc motor. Iraqi J Comput Commun Control Syst Eng 20(3): 29-41. doi: 10.33103/uot.ijccce.20.3.3.

SALMAN MA & KADHIM SK. 2022. Optimal backstepping controller design for prosthetic knee joint. J Eur Syst Automat 55(1): 49-59. doi: 10.18280/jesa.550105.

SERGEY J, SERGEI S & ANDREY Y. 2016.Comparative analysis of iterative LQR and adaptive PD controllers for a lower limb exoskeleton. In: Proceedings of the 2016 IEEE International Conference on Cyber Technology in Automation, Control, and Intelligent Systems (CYBER), Chengdu, China, p. 239-244.

SU H, ENAYATI N, VANTADORI L, SPINOGLIO A, FERRIGNO G & DEMOMI E. 2018. Online human-like redundancy optimization for tele-operated anthropomorphic manipulators. Int J Adv Robot Syst 15: 1-13. doi: 10.1177/1729881418814695.

SUN W, LIN JW, SU SF, WANG N & ER MJ. 2020. Reduced Adaptive fuzzy decoupling control for lower limb exoskeleton. IEEE Trans Cybern 51: 1099-1109. doi: 10.1109/TCYB.2020.2972582.

SUN Z, ZHENG J, MAN Z, WANG H & LU R. 2017. Sliding Mode-Based Active Disturbance Rejection Control for Vehicle Steer-by-Wire Systems. IET Cyber Phys Syst Theory Appl 3(1): 1-10. doi: 10.1049/iet-cps.2016.0013.

TENG L & BAI S. 2019. Fuzzy sliding mode control of an upper-limb exoskeleton robot. In: Proceedings of the 2019 IEEE International Conference on Cybernetics and Intelligent Systems (CIS) and IEEE Conference on Robotics, Automation and Mechatronics, p. 12-17. doi: 10.1109/CIS-RAM47153.2019.9095811.

WANG L, DU Z, DONG W, SHEN Y & ZHAO G. 2018. Intrinsic sensing and evolving internal model control of compact elastic module for a lower extremity exoskeleton. Sensors 18(3): 1-23. doi: 10.3390/s18030909.

WANG F, LIU P, JING D, LIU B, PENG W, GUO M & XIE ML. 2021. Sliding Mode Robust Active Disturbance Rejection Control for Single-Link Flexible Arm with Large Payload Variations. Electronics 10: 1-15. doi: 10.3390/electronics10232995.

WINTER DA. 2009. Biomechanics and Motor Control of Human Movement, Fourth Edition. New Jersey: J Wiley & Sons. doi: 10.1002/9780470549148.

ZHAO X, WANG X, ZHANG S & ZONG G. 2018. Adaptive neural backstepping control design for a class of nonsmooth nonlinear systems. IEEE Trans Syst Man Cybern Syst 49: 1-12.

How to cite
ALAWAD NA, HUMAIDI AJ & ALARAJI AS. 2023. Sliding Mode-Based Active Disturbance Rejection Control of Assistive Exoskeleton Device for Rehabilitation of Disabled Lower Limbs. An Acad Bras Cienc 95: e20220680. DOI 10.1590/0001-3765202320220680.

Manuscript received on August 8, 2022;
accepted for publication on September 16, 2022

NASIR A. ALAWAD[1,2]
https://orcid.org/0000-0003-3059-4375

AMJAD J. HUMAIDI[2]
https://orcid.org/0000-0002-9071-1329

AHMED S. ALARAJI[3]
https://orcid.org/0000-0003-2568-9812

[1]Department of Computer Engineering, Faculty of Engineering, Mustansiriyah University, Palestine Al-Waziriyah Street, 10073 Baghdad, Iraq
[2]Department of Control and System Engineering, University of Technology, Al-Sinaa Street, 10066 Baghdad, Iraq
[3]Department of Computer Engineering, University of Technology, Al-Sinaa Street, 10066 Baghdad, Iraq

Correspondence to: **Nasir A. Alawad**

E-mail: cse.20.33@grad.uotechnology.edu.iq

Author contributions

Nasir A. Alawad designed the study, participated in the sampling, data collection and analysis of samples, and wrote a preliminary version of the manuscript. Amjad J. Humaidi designed the study, work on data interpretation and wrote a final version of the manuscript. Ahmed S. Alaraji was responsible for sample preparation, analysis and collaborate on writing the manuscript. Amjad J. Humaidi worked on data interpretation, writing the manuscript and reviewed it.